Thermal lens study of the Tris(2,2'-bipyridyl)iron(II) tetrafluoroborate

M. D. Zidan[1]*, M. M. Al-Ktaifani[2], M. S. EL-Daher[3], A. Allahham[1], and A. Ghanem[3]

1. Department of Physics, Atomic Energy Commission, Damascus P. O. Box 6091, Syria

2. Department of Radioisotopes, Atomic Energy Commission, Damascus P. O. Box 6091, Syria

3. Higher Institute for Laser Research and Applications, Damascus University, Syria

(Received 11 February 2020; Revised 23 March 2020)

Experimental results of thermal lens measurements for Tris(2,2'-bipyridyl)iron(II) tetrafluoroborate solution are reported using the dual beam technique. The temporal evaluation of thermal lens was observed at input pump power of I=47 mW. The thermal lens effect was observed with increasing the pump power intensity as well. The evolution time of thermal lens and the fitting of the experimental transient curve were useful to evaluate the parameters of the Tris(2,2'-bipyridyl)iron(II) tetrafluoroborate solution.

Document code: A **Article ID:** 1673-1905(2021)03-0183-4

DOI https://doi.org/10.1007/s11801-021-0020-y

Thermal lensing effect occurs when a Gaussian laser beam interacts with nonlinear absorbing medium as a result of local heating of an absorbing medium. The local heating produces a gradient re-distribution in the medium temperature, making a change of refractive-index which known as the thermo-optic coefficient (dn/dT). This makes the heated sample as artificial lens for the incoming laser beam[1]. The evolution of thermal lens happens over short time as the laser beam becomes in thermal equilibrium state with the absorbing sample. Usually, in liquid the refractive-index varies with density decreases and increasing temperature. Then, the term dn/dT is negative, and the thermal lens is considered to be diverging lens[2]. That means in the case of the negative lens the laser beam will be spreading and the intensity of the beam will be dropped. By measuring the change in the laser intensity beyond the sample, some information related to the thermo-optic[3], and nonlinear optical properties of the studied materials can be obtained[4]. A theoretical model based on the laser-induced thermal lens effect in absorbing media was fully explained in Refs.[1, 5—7]. The thermal lens technique is well known method to determine the thermo-optic coefficient (dn/dt) and other nonlinear parameters of the studied sample. These parameters may help as effective optical tools for evaluating impure compounds[8]. An extensive works have been done to investigate the thermal lens effect of different materials utilizing the thermal lens technique using single laser beam with chopper to predict the time evolution of the thermal lens case[7]. Other researchers have used the dual pump-probe configuration to study the thermal lens properties in organic molecules[8-10].

In addition to our recent work on the Tris(2,2'-bipyridyl)iron(II) tetrafluoroborate solution[11], we present the experimental investigation of thermal lens effect in the Tris(2,2'-bipyridyl)iron(II) tetrafluoroborate solution employing the dual beam (pump-probe) configuration.

The Tris(2,2'-bipyridyl)iron(II) tetrafluoroborate was already prepared and characterized by earlier work[11]. Fig.1 shows the schematic diagram of the pump-probe experimental setup. It consists of modulated diode pump solid state laser "MGL-H-532/500" with a maximum power up to 500 mW used as an excitation pump source, and probe laser beam (TEM_{00} Gaussian) comes from the stabilize He-Ne (Thornlab), λ=632.8 nm with power of 1 mW to scan the sample for investigating thermal lens effect. The angle between the incident probe laser and the pump beam was calculated to be (α≈1.4°). The probe beam waist is three times larger than that of the pump. The shape of the weak probe beam has a Gaussian profile; the distribution power of laser beam profile has been recorded by CCD camera. The probe beam signal is directed to the detector (silicon photo-detector from Thornlab DET-110) which is connected to digital oscilloscope.

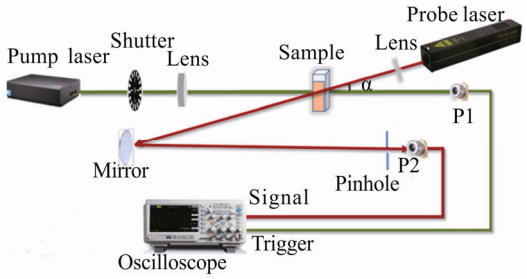

Fig.1 The thermal lens experimental setup

* E-mail: pscientific8@aec.org.sy

A closed-aperture *z*-scan measurement was performed using a CW laser with a wavelength of 532 nm for the Tris(2,2'-bipyridyl)iron(II) tetrafluoroborate in ethanol with concentration of 10^{-3} M. Fig.2 shows the transmitted intensity of the sample solution at different *z*-position (pure nonlinear refraction index curve). The feature of the recorded curve is a peak to valley configuration, which tells about the sample behavior; it is consider being self-defocusing materials. Thus, the sample behaves as a negative lens, which could diverge and makes distortion to the probe beam. Fig.2 indicates that the length between the peak-valley ($\Delta z_{p\text{-}v}$) is larger than $1.7\times Z_R$, where Z_R=4.176 mm. This refers that the thermal lens mechanism is applicable to our study[12,13]. However, the physical origin of the nonlinear refractive index could be thermal in nature due to the laser source which is a CW laser[14,15].

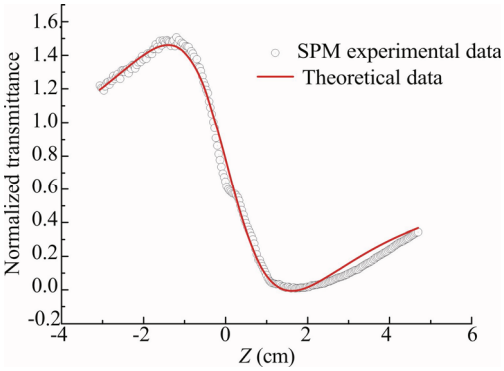

Fig.2 The pure closed aperture *z*-scan data at *λ*=532 nm

Fig.3 displays the 2-D probe laser spot passed through the sample without pump beam and the same laser spot with pump laser beam. This gives strong evidence to the formation of the thermal lens in the presence of pump beam at 17.4 mW.

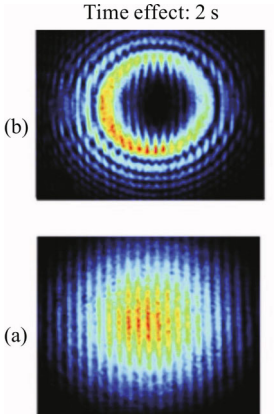

Fig.3 (a) The probe laser spot without pump laser beam; (b) The probe laser spot with pump beam in the sample

In order to evaluate the thermal lens effect of the sample structure, we have recorded the thermal lens image for pure ethanol solvent and with sample solution at pump power 43 mW, and Fig.4 shows the difference between the two cases.

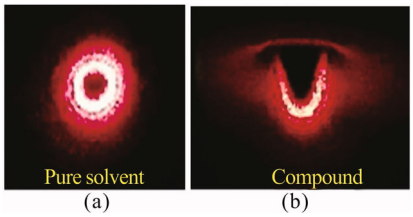

Fig.4 The thermal lens images of probe laser (a) with solvent only and (b) with the sample solution

On next step, we have recorded the thermal lens image as three dimensional profiles with different input pump laser powers at: 0 mW (without thermal lens effect), 8.90 mW, 17.40 mW, 27.80 mW and 47.30 mW using CCD camera. This procedure will help us to recognize the mechanism of the development of the thermal lens image with change of the input pump power. The size of the top hollow regions was inspected as seen in Fig.5. It can be seen from the figure that the top hollow region in the middle of the probe laser beam is increased with the input laser pump power[9-16]. Our results have shown that the shape of the probe beam is changed from Gaussian at low pump beam power to a near-doughnut shape at higher pump beam powers. Therefore, the thermal lens medium can change the quality (Gaussian shape) of a probe beam which propagates through this medium.

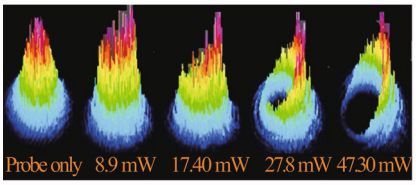

Fig.5 Three dimensional images of the thermal lens effect captured by the CCD camera at different pump powers

Fig.6 shows the temporal evolution of thermal lens, when the pump power is 47 mW using a beam profiler. The thermal lens effect develops through a period of time controlled by the rise time of the pump beam and characteristic of the thermal time constant of the medium[17]. We can characterize the temporal evolution of the thermal lens as follows: At *t*=0 ms no thermal lens appears, from 500 ms to 3 000 ms, the thermal lens having symmetrical circular feature and the thermal conduction processes predominate. Then, at larger time than 3 000 ms, the shape of the thermal lens starts to change as a hollow area, with the diameter of the hollow becomes larger the time.

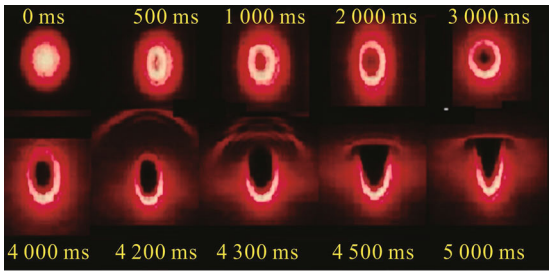

Fig.6 The temporal evaluation of thermal lens at input pump power *I*=47 mW

It should be mentioned here that the thermal lens transient experiment was done using the dual beam (pump-probe beams configuration). A mechanical chopper (with frequency of 0.5 Hz) was located in the laser beam way to modulate the pump laser beam for getting time resolved measurement.

Fig.7 depicts the thermal lens transient signal for the studied sample using a weak probe laser beam at 1 mW and the pump power up to 50 mW. The inset in Fig.7 shows the image of the pump laser beam transmission when the thermal lens is induced in the presence of the mechanical chopper. The fitting curve was obtained by applying the experimental data (Fig.7) to the thermal lens signal equation[18,19]:

$$I(t) = I(0)\left[1 - \frac{\theta}{2} \times \tan^{-1}\left(\frac{2mV}{[(1+2m)^2 + V^2]\frac{t_c}{2t} + 1 + 2m + V^2}\right)\right]^2, \quad (1)$$

where t_c and θ are adjustable parameters could be obtained by fitting the above formula, where $m = (\frac{\omega_{1p}}{\omega_e})^2$, and ω_{1p} and ω_e are the radii of the probe beam and pump beam in the sample, respectively. Also, $V \approx (\frac{Z_1}{Z_c})$, when $Z_2 >> Z_c$, where Z_1 is the distance between the waist of probe laser beam and the sample position, Z_2 is the length between the sample and the detector position in far field, $Z_c = \frac{\omega_0^2}{\lambda}$, and $I(0)$ is the value of $I(t)$ when t or θ is zero.

The characteristic thermal time of the medium is determined with the following equation:

$$t_c = \frac{\omega_e^2}{4D}, \quad (2)$$

where ω_0 is the beam radius inside the sample, and D is the thermal diffusivity (cm^2/s):

$$D = \frac{k}{\rho c}, \quad (3)$$

where k is thermal conductivity, ρ is the sample density and c is the specific heat of the studied sample.

The phase distortion probe θ related to the thermo-optic coefficient as follows:

$$\theta = -\frac{P_e \alpha_0 L_{eff}}{k\lambda_p}\frac{dn}{dt}. \quad (4)$$

For the thermal nonlinearity and steady state case, the on-axis change in the refractive index Δn can be given as[20]

$$\Delta n = \frac{dn}{dT}\frac{I\alpha_0\omega_o^2}{4k}, \quad (5)$$

and

$$\Delta n = n_2 I, \quad (6)$$

where n_2 is the nonlinear refractive index and I is the laser intensity.

Using the above equations, we have calculated the values of the following parameters θ, t_c, D, dn/dt, n_2 and Δn of the Tris(2,2'-bipyridyl)iron(II) tetrafluoroborate solution, and they are given in Tab.1. Our present results are in reasonable agreements with similar works[3, 21-23] as seen in Tab.1.

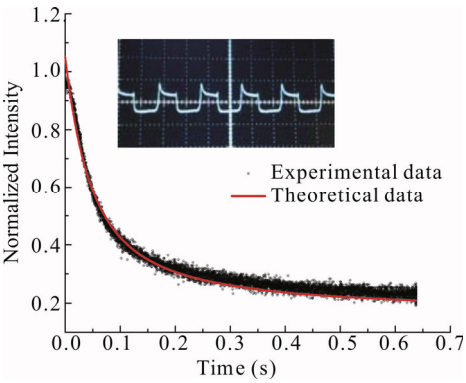

Fig.7 Transient signal for the Tris(2,2'-bipyridyl)iron(II) tetrafluoroborate solution

Tab.1 The calculated parameters of the Tris(2,2'-bipyridyl)iron(II) tetrafluoroborate solution

Sample	Θ (rad)	t_c (s)	D (cm^2/s)	dn/dt (k^{-1})	n_2 (cm^2/W)	$\Delta n \times 10^{-4}$
Tris(2,2'-bipyridyl)iron(II) tetrafluoroborate (Our present results)	1.27	0.015	5×10^{-3}	-2.11×10^{-6}	-8.46×10^{-8}	-1.69
Zinc sulfide nanoparticles[21]	-	-	-	-4.83×10^{-5}	66.87×10^{-5}	-
Tm^{3+}-doped telluriteglasses[22]	0.075	0.002	2.62×10^{-3}	-0.13×10^{-5}	3.89×10^{-13}	-
PMMA base containing BCP[23]	2.63	0.004	4.46×10^{-5}	-5.54×10^{-5}	6.24×10^{-7}	-1.36
Azomethine in chloroform[3]	0.95	0.031	3.92×10^{-5}	-71.7	-32.6×10^{-8}	-

We observed thermal lens effect using the dual pump-probe configuration. The thermal lens linearly increased with intensity. The effect of the pump laser power on the probe beam shape and its quality was observed. Our work has shown that the thermal lens effect increases with the pump laser power as a result deforms the probe beam profile. The temporal evaluation time of the thermal lens was observed with the time at fixed input pump power.

Acknowledgements

The authors would like to thank Prof. I. Othman, Director General, Prof. M. K. Sabra and Prof. A. H. Al-Rayyes, Head of the Radioisotope Department for their support.

References

[1] Wang Y., Tang Y., Cheng P., Zhou X., Zhu Z., Liu Z. and Bao J., Nanoscale **9**, 3547 (2017).
[2] Karimzadeh R., J. Opt. **14**, 095701 (2012).
[3] Hussain A. Badran, Appl. Phys. B **119**, 319 (2015).
[4] Jia Y., LI Z., Saeed M., Tang J., Cai H. and Xiang Y., Optics Express **27**, 20857 (2019).
[5] Salmani S. and Ara M. H. M., Optics & Laser Technology **82**, 34 (2016).
[6] Mahdieh M. H. and Akbari Jafarabadi M., Optics & Laser Technology **44**, 78 (2012).
[7] Karimzadeh R. and Arshadi M., Laser Phys. **23**, 115402 (2013).
[8] Pilla V., Munin E. and Gesualdi M. R. R., J. Opt. A: Pure Appl. Opt. **11**, 105201 (2009).
[9] Mahdieh M. H., Jafarabadi M. A. and Ahmadinejad E., Proc. of SPIE **9255**, 925531 (2015).
[10] Rohling J. H., Mura J., Pereira J. R. D. and Palangana A. J., Brazilian Journal of Physics **32**, 575 (2002).
[11] Zidan M. D., Al-Ktaifani M. M. and Allahham A., Optics & Laser Technology **90**, 174 (2017).
[12] Cuppo F. L. S. A., A. Neto M. S F., Gomez S. L. and Palffy-Muhoray P., J. Opt. Soc. Am. B **19**, 1342 (2002).
[13] Nóvoa-López J. A., López Lago E., Domínguez-Pérez M., Troncoso J., Varela L. M., R.de la Fuente, Cabeza O., Michinel H. and Rodríguez J. R., Optics & Laser Technology **61**, 1 (2014).
[14] Rita S. Elias, Qusay M. A. Hassan, C. A. Emshary, H. A. Sultan and Bahjat A. S., Spectrochimica Acta Part A: Molecular and Biomolecular Spectroscopy **223**, 117297 (2019).
[15] Zidan M. D., Al-Ktaifani M. M. and Allahham A., Journal of Optoelectronics and Advanced Materials **21**, 93 (2019).
[16] Santhi A. J, Misha H., Mathew S., Gaurav S., Soumya Hadiya V. M., Radhakrishnan P. and Nampoori V. P. N., Opt. Commun. **283**, 313 (2010).
[17] Badran H. A., Results in Physics **4**, 69 (2014).
[18] Shen J, Baesso ML and Snook RD, Appl. Phys. **75**, 3738 (1994).
[19] Pilla V, Chillcce E F, Neves AAR, Munin E, Catunda T and Cesar CL, J. Mater. Sci. **42**, 2304 (2007).
[20] Qusay M. A. Hassan, Hussain A. Badran, Alaa Y. AL-Ahmad and Chassib A. Emshary, Chin. Phys. B **22**, 114209 (2013).
[21] Alfahed R. K. F., Al-Asadi A. S., Badran H. A. and Ajeel K. I., Applied Physics B **125**, 48 (2019).
[22] Seshadri M., Radha M., Darabian H., Barbosa L. C., Bell M. J. V. and Anjos V., Journal of Thermal Analysis and Calorimetry **138**, 2971 (2019).
[23] Badran H. A., Al-Fregi A. A., Alfahed R. K. F. and Al-Asadi A. S., Journal of Materials Science: Materials in Electronics **28**, 17288 (2017).